Available online at www.sciencedirect.com

ScienceDirect

Procedia Manufacturing 35 (2019) 854–860

Procedia MANUFACTURING

www.elsevier.com/locate/procedia

2nd International Conference on Sustainable Materials Processing and Manufacturing (SMPM 2019)

Environmental Effect of Corrosion on Meteorological Parameters Over Malabo

Emetere M.E.[a,b*] and Olawole O.C. [a]

[a]*Department of Physics, Covenant University Canaan land, P.M.B 1023, Ota, Nigeria.*
[b]*Department of Mechanical Engineering Science, University of Johannesburg, South Africa.*

Abstract

Recent research works have shown how climate change has affected atmospheric corrosion of metallic surfaces. A mathematical model was developed to study the impact of atmospheric corrosion (aerosol) over fifteen years primary dataset (Multi-angle Imaging Spectro-Radiometer). From the primary dataset, an estimation of the aerosol loading, size of particulates and angstrom exponent was presented. The yearly corrosion rate has doubled in recent time, hence confirming the impact of climate change on atmospheric corrosion. Higher accuracy of the modified Faraday model can be achieved using ground dataset.

Peer-review under responsibility of the organizing committee of SMPM 2019.

Keywords: aerosol, aerosol loading, corrosion, atmospheric corrosion

1. Introduction

Corrosion is initiated when metallic surfaces have contact with natural and artifical atmospehric aerosol [1-2]. This corrosion is an unavoidable phenomenon because metal production requires continuous energy gain into the system which may cause the metals to posesses low Gibbs energy. Therefore, when a system assumes the state of low Gibbs energy, the system is susceptible to corrosion. In general terms the negative impact of atmospheric corrrosion (aerosol) is caused by condensed nature of the humidity, capillarity, chemical and the nature of aqueous precipitation [2-3]. The adoption of thermodynamic principle to the study of metal corrosion has revealed its cost implication on industry [1]. Figure 1 shows the maintenace cost of corrosion in the United State.

* Corresponding Author
Email: emetere@yahoo.com

2351-9789
Peer-review under responsibility of the organizing committee of SMPM 2019.
10.1016/j.promfg.2019.07.016

Researchers have identified that atmospheric sorrosion is largely dependent on surface exposure duration, rust characteristics, temperature, atmospheric pollution and metal components[4-5]. Hence, it is possible that climate change may have influenced atmospheric corrosion in recent time. Atmospheric corrosion (aerosol) comprise of the oxidation and reduction processes:

Oxidation of the metal (anodic reaction)

$$Fe \rightarrow Fe^{2+} + 2e^{-} \quad (1)$$

Reduction of the oxygen (cathodic reaction)

$$0_2 + 2H_20 + 4e^{-} \rightarrow 4OH^{-} \quad (2)$$

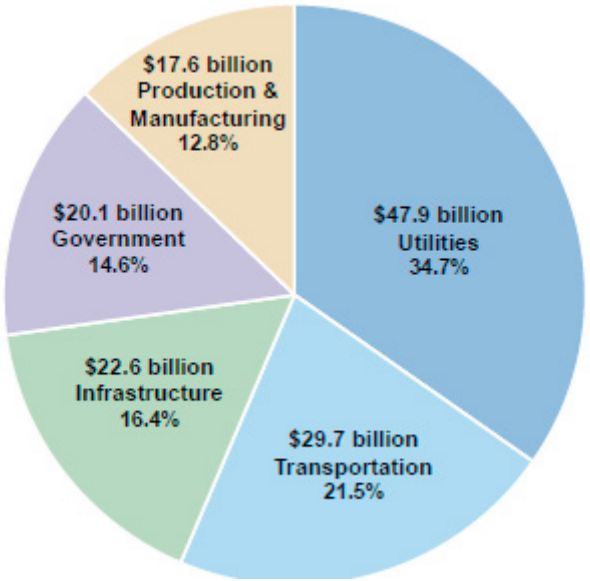

Figure 1: Cost intensiveness of corrosion on US economy[6]

2. Materials and Methods

The research location is Malabo, Equitoria Guinea which lies on longitude and latitude of 8.7371° E and 3.7504° N respectively (Figure 2). The West African regional scale dispersion model (WASDM) was used to estimate the aerosol loading over a region. WASDM for aerosol loading is given as [8-10]:

$$\psi(\lambda) = a_1{}^2 \cos\left(\frac{n_1 \pi \tau(\lambda)}{2} x\right) \cos\left(\frac{n_1 \pi \tau(\lambda)}{2} y\right) + \cdots \ldots a_n{}^2 \cos\left(\frac{n_n \pi \tau(\lambda)}{2} x\right) \cos\left(\frac{n_n \pi \tau(\lambda)}{2} y\right) \quad (3)$$

a is atmospheric constant gotten from the fifteen years aerosol optical depth (AOD) dataset from MISR, n is the tunning constant, $\tau(\lambda)$ is the AOD of the area and $\psi(\lambda)$ is the aerosol loading.

The digital voltage and Angstrom parameters of the study area can be obtained from equations (4) and (5) respectively.

$$I(555) = \frac{I_o(555)}{R^2} \exp(m * \tau(555)) \quad (4)$$

where I s the solar radiance over the SPM detector at wavelength λ = 555 nm, Io is the is a measure of solar radiation behind the atmosphere, R is the mean Earth-Sun distance in Astronomical Units, τ is the total optical

depth (in this case, the average of the each month is referred to as the total AOD, and m is the optical air mass.

$$\alpha = -\frac{\mathrm{d\ In}\ (\tau)}{\mathrm{d\ In}\ (\lambda)} \tag{5}$$

where α is the Angstrom parameter, τ is the aerosol optical depth, and λ is the wavelength. The radius of the particles for atmospheric aerosol and back-envelope was calculated using proposals by Kokhanovsky et al [11]. The analysis of equations (1) was done using the C++ codes.

The atmospheric corrossion rate of metals over the Dori was calculated using the Faraday equation [12]. It is given as :

$$CR\ \left(\frac{\mu m}{yr}\right) = k\frac{i_{corr}}{d}EW \tag{6}$$

Where k is a conversion factor (3.27 x 10^6 μm·g·A^{-1}·cm^{-1}·yr^{-1}), i_{corr} is the corrosion current density in μA/cm² (calculated from the measurements of Rp), EW is the equivalent weight, and d is the density of Alloy 22 (8.69 g/cm³).

Based on equation (6), the modification in the work is the inclusion of aerosol loading.

$$CR\ \left(\frac{\mu m}{yr}\right) = k\frac{i_{corr}}{d}EW/\exp\left(\frac{\mathrm{EW}^{*}\psi(\lambda)}{2.32}\right) \tag{7}$$

In this study, the corrosion current density of iron was considered and it is given as 3.2 x10^{-3} μA/cm². The EW of iron is given as 27.9225.

Figure 2: Google map of Malabo

3. Results and Discussion

The graph of the aerosol optical depth (AOD) is presented in Figure 3. It is observed that the highest AOD over fifteen years were in 2004 and 2006. The radius of particle (back of envelope calculation) is presented in Figure 3. The aerosol loading that was derived from the West African regional scale dispersion model (WASDM) is presented in Figure 4. The dataset of the aerosol loading show the cumulative effect of aerosols emission over an area. At the moment the aerosol loading over Malabo is considered high. The aerosol sizes over Malabo is presented in Table 1. The statistics of the AOD data presented in Table 2. The corrosion rate over Malabo on iron metallic surfaces is presented in Figure 5. The corrosion rate over Malabo is high and confirms the earlier ascertion that climate change has influence over atmospheric corrosion.

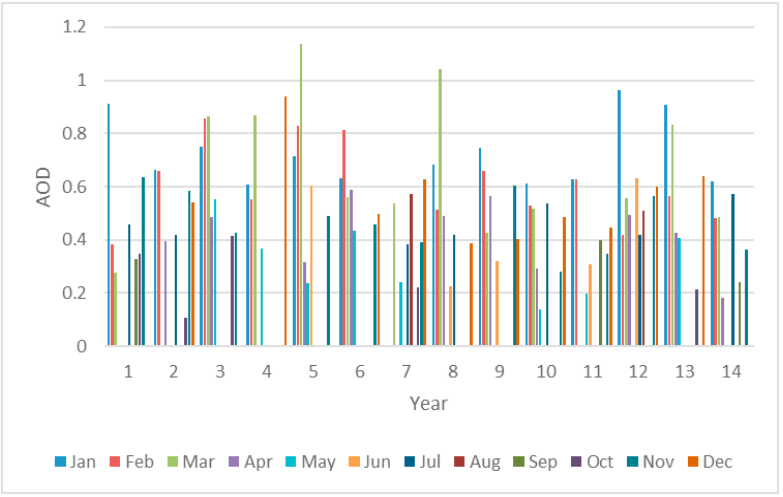

Figure 3: Aerosol optical depth over Malabo between years 2000 and 2013

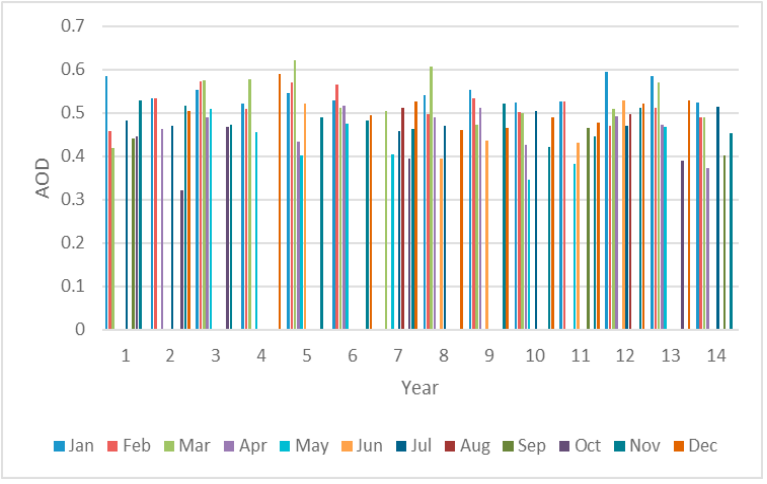

Figure 4: Radius of particulate-back of envelope calculation between years 2004 and 2013

Table 1: Radius of particulate-atmospheric aerosols between years 2000 and 2004

Month	2000	2001	2002	2003	2004	2005	2006	2007	2008	2009	2010	2011	2012	2013
Jan	7.91E-07	6.72E-07	7.14E-07	6.45E-07	6.98E-07	7.58E-07		6.82E-07	7.12E-07	6.47E-07	6.55E-07	8.14E-07	7.88E-07	6.51E-07
Feb	5.29E-07	6.70E-07	7.63E-07	6.18E-07	7.51E-07	7.97E-07		5.98E-07	6.70E-07	6.06E-07	6.55E-07	5.48E-07	6.24E-07	5.83E-07
Mar	4.69E-07		7.68E-07	7.70E-07	8.95E-07	7.41E-07	6.11E-07	8.51E-07	5.53E-07	6.00E-07		6.19E-07	7.54E-07	5.84E-07
Apr		5.37E-07	5.84E-07		4.91E-07	7.48E-07		5.85E-07	6.24E-07	4.78E-07		5.89E-07	5.52E-07	4.05E-07
May			6.18E-07	5.22E-07	4.43E-07	7.04E-07	4.46E-07			3.71E-07	4.15E-07		5.43E-07	
Jun					6.44E-07			4.35E-07	4.93E-07		4.87E-07	6.57E-07		
Jul	5.70E-07	5.48E-07					5.29E-07	5.50E-07		6.10E-07		5.49E-07		6.28E-07
Aug							6.27E					5.95E		

							-07					-07		
Sep	4.99E -07										5.39E -07			4.44E -07
Oct	5.10E -07	3.40E -07	5.46E -07				4.31E -07						4.27E -07	
Nov	6.59E -07	6.33E -07	5.53E -07		5.85E -07	7.12E -07	5.34E -07		6.43E -07	4.71E -07	5.10E -07	6.24E -07		5.19E -07
Dec		6.11E -07		8.03E -07		7.23E -07	6.55E -07	5.30E -07	5.41E -07	5.83E -07	5.63E -07	6.42E -07	6.60E -07	

Table 2: AOD statistics over Malabo between years 2005 and 2009

Statistics	**2005**	**2006**	**2007**	**2008**	**2009**
Number of values	7.000	7.000	7.000	7.000	8.000
Number of missing values	5.000	5.000	5.000	5.000	4.000
Minimum	0.569	0.424	0.536	0.532	0.424
First quartile	0.467	0.277	0.393	0.410	0.287
Third quartile	0.621	0.563	0.641	0.645	0.533
Standard error	0.049	0.060	0.099	0.058	0.058
95% confidence interval	0.119	0.148	0.243	0.142	0.137
99% confidence interval	0.180	0.224	0.368	0.215	0.203
Variance	0.016	0.026	0.069	0.024	0.027
Average deviation	0.093	0.132	0.186	0.127	0.139
Standard deviation	0.128	0.160	0.263	0.153	0.164
Coefficient of variation	0.226	0.377	0.490	0.288	0.387
Skew	1.133	-0.100	1.250	-0.036	-0.768
Kurtosis	1.420	-1.710	2.052	-1.302	-0.756
Kolmogorov-Smirnov stat	0.170	0.190	0.251	0.182	0.268
Critical K-S stat, alpha=.10	0.436	0.436	0.436	0.436	0.410
Critical K-S stat, alpha=.05	0.483	0.483	0.483	0.483	0.454
Critical K-S stat, alpha=.01	0.576	0.576	0.576	0.576	0.542

Table 3: AOD statistics over Malabo between years 2010 and 2013

Statistics	**2010**	**2011**	**2012**	**2013**
Number of values	7.000	9.000	7.000	7.000
Number of	5.000	3.000	5.000	5.000

missing values				
Mean	0.422	0.573	0.570	0.421
First quartile	0.318	0.476	0.411	0.270
Third quartile	0.582	0.609	0.785	0.550
Standard error	0.061	0.055	0.093	0.062
95% confidence interval	0.149	0.126	0.228	0.153
99% confidence interval	0.225	0.184	0.345	0.231
Variance	0.026	0.027	0.061	0.027
Average deviation	0.124	0.106	0.192	0.136
Standard deviation	0.161	0.164	0.246	0.165
Coefficient of variation	0.381	0.287	0.432	0.392
Skew	0.236	1.875	0.071	-0.402
Kurtosis	-0.951	4.464	-0.915	-1.360
Kolmogorov-Smirnov stat	0.185	0.247	0.151	0.219
Critical K-S stat, alpha=.10	0.436	0.387	0.436	0.436
Critical K-S stat, alpha=.05	0.483	0.430	0.483	0.483
Critical K-S stat, alpha=.01	0.576	0.513	0.576	0.576

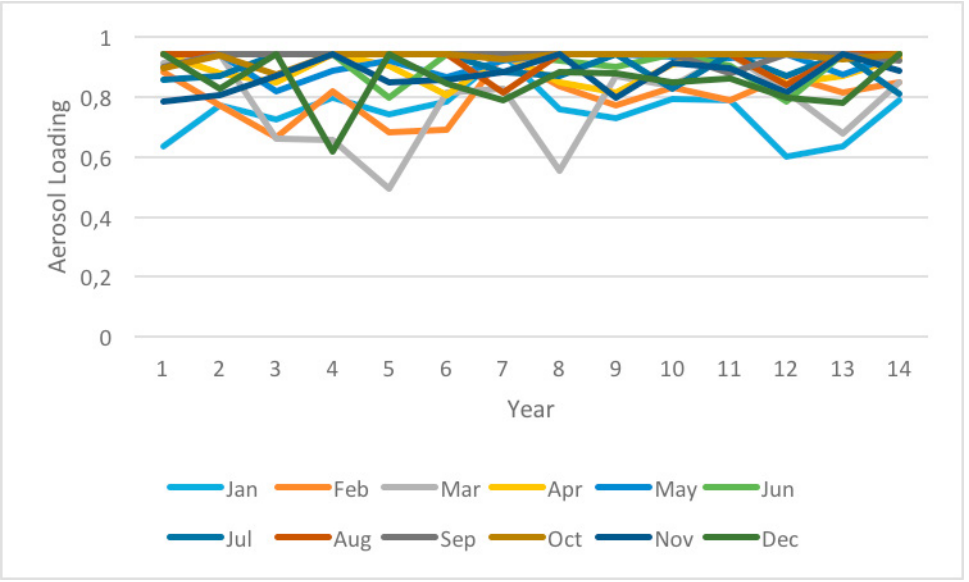

Figure 5: Aerosol loading over Malabo between years 2000 and 2013

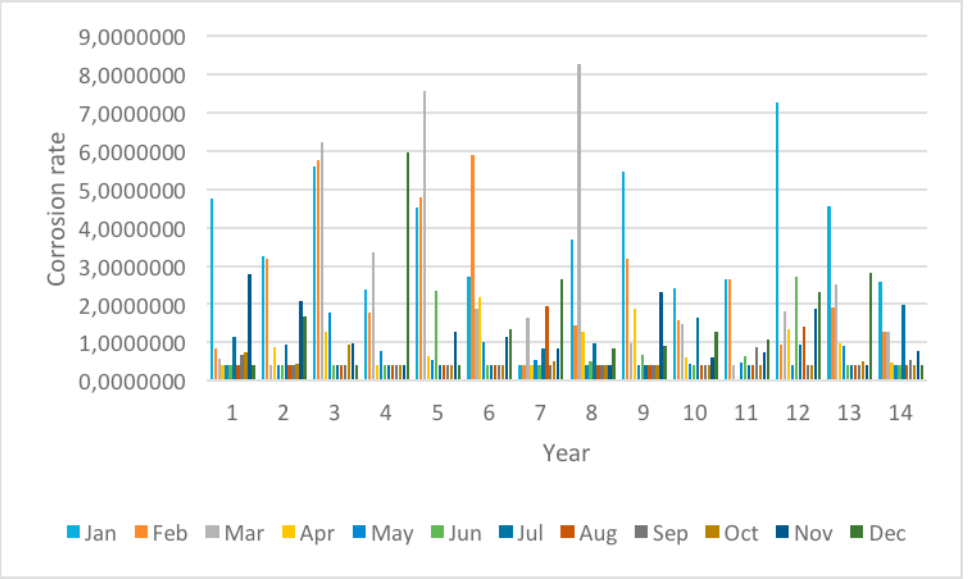

Figure 6: Yearly corrosion rate over Malabo between years 2000 and 2013

4. Conclusion

The yearly corrosion rate has almost doubled since 2004. Hence, atmospheric corrosion in regions of high aerosol loading is high. Higher accuracy of the modified Faraday model can be achieved using ground dataset.

Acknowledgements

The authors wish to appreciate their institutions. The authors acknowledge NASA for primary dataset.

References

[1]. Emetere Moses E., Akinyemi M.L. & Oladimeji T.E. (2016) Statistical Examination Of The Aerosols Loading Over Kano, Nigeria: The Satellite Observation Analysis, Scientific Review Engineering and Environmental Sciences, 72: 167-176
[2]. Emetere M.E., Akinyemi M.L., & Akinojo O., (2015) Parametric retrieval model for estimating aerosol size distribution via the AERONET, LAGOS station, Environmental Pollution, 207 (C), 381-390
[3]. Emetere, Moses Eterigho, (2016) Statistical Examination of the Aerosols Loading Over Mubi-Nigeria: The Satellite Observation Analysis, Geographica Panonica, 20(1), 42-50
[4]. Moses Eterigho Emetere, (2017). Investigations on aerosols transport over micro- and macro-scale settings of West Africa, Environ. Eng. Res., 22(1), 75-86
[5]. M. E. Emetere, (2017). Impacts of recirculation event on aerosol dispersion and rainfall patterns in parts of Nigeria, GLOBAL NEST JOURNAL 19 (2), 344-352
[6]. Rosa Vera, Diana Delgado, Blanca Rosales, Corros. Sci. 50 (2008) 1080-1098.
[7]. Rosa Vera, Patricia Verdugo, Marco Orellana, Eduardo Muñoz, Corros. Sci. 52 (2010) 3803-3810
[8]. H.C. Vasconcelos, B.M. Fernández-Pérez, J. Morales, R.M. Souto, S. González, V. Cano, and J.J. Santana (2014). Development of Mathematical Models to predict the Atmospheric Corrosion Rate of Carbon Steel in Fragmented Subtropical Environments, Int. J. Electrochem. Sci., 9: 6514 -6528
[9]. A.A. Kokhanovsky, W. Von Hoyningen-Huene, J.P. Burrows, Atmospheric aerosol load as derived from space, Atmospheric Research, 81 (2006), pp. 176-185
[10]. ASTM International, Volume 03.02, Standards G 5, G 48, G 59, G 61, G 102 (ASTM International, 2003: West Conshohocken, PA).